Estimation of Phosphate Extractability in Flooded Soils: Effect of Solid-Solution Ratio and Bicarbonate Concentration

Mitra Amini[a], Juan Antelo[b], Sarah Fiol[b,c], Rasoul Rahnemaie[a,*]

[a] Department of Soil Science, Tarbiat Modares University, P.O. Box 14115-336, Tehran, Iran

[b] CRETUS. Department of Soil Science and Agricultural Chemistry, University of Santiago de Compostela, 15782 Santiago de Compostela, Spain

[c] CRETUS. Department of Physical Chemistry, University of Santiago de Compostela, 15782, Santiago de Compostela, Spain

[*]**Corresponding Author:** rahnemaie@modares.ac.ir; +98 21 48292278

Abstract

The Olsen method is widely used to determine bioavailable or extractable phosphate (P) in upland soils. It is also used in flooded soils, although different estimates of extractable P are obtained under anoxic conditions and oxic conditions. In the present study, variations in extractable P in three soils under different redox conditions were evaluated as a function of solid to solution ratio (SSR) (1:5-1:200) and bicarbonate concentration (0.1-1 M). The parameterized CD-MUSIC model was used to describe the data, with optimization of reactive surface area (RSA) and reversibly adsorbed P (R-PO_4) only. The RSA may vary due to the reductive dissolution of iron minerals and/or the formation of new reactive surfaces upon the establishment of reducing conditions. Changes in SSR and bicarbonate concentration significantly affected extractable P under both oxic and anoxic conditions; more P was extracted under anoxic conditions than under oxic conditions. The difference was 1.5 to 2 times greater for the highest SSR considered. In the soil samples with higher organic carbon content, the effect of bicarbonate concentration on extractable P was remarkable. The large differences in extractable P under oxic and anoxic conditions were probably due to differences in iron (hydr)oxide content. The parameterized CD-MUSIC model successfully predicted the effect of SSR on extractable P under oxic and anoxic conditions. R-PO_4 data were fitted for oxic conditions and assumed unchanged for anoxic samples, while RSA data were fitted for both conditions. The RSA value was lower in anoxic samples than in oxic samples. Overall, our experimental data and model calculations indicate that using wet soil samples obtained in situ for evaluation of Olsen-P in submerged soils leads to estimation of higher amounts of extractable P than estimated in oxic soils. If soil testing in the presence of target plants confirms the reliability of in-situ sampling for Olsen-P estimation, the P

fertilizer dose applied to submerged soils could be reduced, which is very important from environmental and economic perspectives.

Keywords: *Anoxic conditions, Extractable phosphate, Iron (hydr)oxides, Organic carbon, Surface complexation modeling*

1. Introduction

Phosphate (P) is an essential nutrient for living organisms. It is commonly applied to agricultural soils as a fertilizer to improve plant yields. A large fraction of the fertilizer applied is either precipitated or strongly bound to soil minerals. Thus, phosphate bioavailability is usually a limiting factor for growth of plants and microorganisms (Pant and Reddy 2001).

In soils, P is present in four major pools: (i) (a small fraction) dissolved in the soil solution, (ii) adsorbed on soil minerals, (iii) precipitated as Al, Fe, and Ca phosphate minerals and (iv) as a constituent of organic matter (Wuenscher et al. 2015). A fraction of the adsorbed phosphate and all of the soluble phosphate are considered readily extractable forms. In calcareous soils, extractable P is often determined by the Olsen method, in which soil samples are placed in contact (non-equilibrium condition) with sodium bicarbonate under oxic conditions (Olsen et al. 1954). This method has also been used in acidic and neutral soils (Barrow and Shaw 1976a, Horta and Torrent 2007, Hiemstra et al. 2010). In the Olsen method, a fraction of the adsorbed phosphate is released into the soil solution due to a competitive reaction with bicarbonate ions. Under the conditions of the Olsen method, dissolved Ca precipitate as $CaCO_3$(s) and the dissolution of highly soluble calcium phosphate is promoted (Braun et al. 2019).

When an extractant releases P into the solution, the P tends to precipitate and/or become re-adsorbed on mineral surfaces. Therefore, the final estimate of the amount of P extracted is the sum of opposing processes. This explains why in experimental assessments, the amount of P extracted varies with pH, solid to solution ratio (SSR), equilibration time, shaking speed, and/or the concentration of the extractant solution (Sibbesen 1983). Because Olsen extraction is a non-equilibrium process, in some studies (Barrow and Shaw 1976a, 1976b, McDowell and Sharpley 2003, Hiemstra et al. 2010), the effects of various factors such as SSR, equilibration time and sodium bicarbonate concentration on the extractable P have been investigated. Results have shown that by increasing any of these factors, the concentration of extracted P increases.

In many countries, the standard Olsen method (with air-dried sample) is widely used to evaluate extractable P in flooded soils, where anoxic conditions may dominantly affect the extractable P due to the dissolution of iron (hydr)oxides (Ponnamperuma 1972, Saeed et al. 2018, Herndon et al. 2020) and/or the formation of poorly crystalline iron oxides. In the latter process, dissolved iron diffuses upwards to the oxidized soil-water interface and is subsequently hydrolyzed and forms new active surfaces for re-adsorption of P (Sah et al. 1989, Shahandeh et al. 1994, Zhang et al. 2003, Tian et al. 2017). Phosphate extractability may also decrease due to the formation of Fe-phosphate minerals such as vivianite ($Fe_3(PO_4)_2.8H_2O$) (Loeb et al. 2008, Cosmidis et al. 2014). Therefore, it seems that applying the standard Olsen method to flooded soils results in different values of extractable P than when measured under oxic conditions, which may be related to changes in the soil solution chemistry, iron (hydr)oxide surfaces and dissolved organic matter concentration.

In the past two decades, surface complexation models (SCMs) have been widely used to describe oxyanion adsorption on (hydr)oxide minerals (Rahnemaie et al. 2007a, Rahnemaie et al. 2007b, Antelo et al. 2010, Weng et al. 2012, Mendez and Hiemstra 2019) and their competition with the organic matter under both oxic (Weng et al. 2008, Hiemstra et al. 2013) and anoxic conditions (Amini et al. 2020). The thermodynamic constants derived from the relatively simple systems can be used to simulate reactions in complex media such as soil systems. These models have been successfully used to describe P interactions in oxic soils (Gustafsson 2001, Devau et al. 2009, Hiemstra et al. 2010, Weng et al. 2011, Mendez et al. 2020a), but have not yet been tested in anoxic soils.

In soils, P is dominantly adsorbed on iron and aluminum (hydr)oxides such as goethite, ferrihydrite and gibbsite, which can be used as proxies for modeling the soil system behavior. An extensive database regarding ion adsorption interactions on ferrihydrite has been compiled in recent years (Antelo et al. 2010, Hiemstra and Zhao 2016, Mendez and Hiemstra 2019, 2020b). We, therefore, made use of these data and considered this mineral as representing soil (hydr)oxide minerals.

Based on the aforementioned points, we believe that using air-dried soil samples for P extraction under anoxic conditions leads to incorrect estimation of P, and in-situ sampling is therefore needed for extraction of P under such conditions. To investigate this hypothesis, this study aimed to (i) compare the extraction of phosphate in oxic and anoxic soil samples using the Olsen method and (ii) simulate extractable P in both oxic and anoxic conditions using surface complexation models (SCMs). To attain these goals, extractable P was first measured as a function of SSR and sodium bicarbonate concentration. The experimental data were then

described by the state-of-the-art CD-MUSIC (Charge Distribution MUlti SIte Complexation) model. The model was parameterized by the ion (H, Na, CO_3, PO_4) adsorption parameters derived in the relatively simple systems.

Ferrihydrite is a weakly crystalline iron oxide mineral and because of its ability to become adsorbed to surfaces, it plays an important role in determining phosphate concentration in soils. For simplification, we assumed that soil reactive minerals act in the same way as the ferrihydrite mineral. In particular, we examined the efficiency of the CD-MUSIC model to describe phosphate interactions in very complicated anoxic soil systems and compared the effect of SSR on extractable P in both oxic and anoxic soil samples.

2. Materials and methods

2.1. Soil sampling

Three soil samples, mainly differing in organic carbon (OC) content, were collected from Mashatook ($S_{0.5}$, contains 0.54 % OC: location 37° 16′ 44″ N 49° 27′ 51″ E), Sangar ($S_{1.7}$, contains 1.72 % OC: location 37° 9′ 0″ N 49° 44′ 17″ E) and Atashgah ($S_{2.9}$, contains 2.87 % OC, location 37° 16′ 3″ N 49° 30′ 12″ E), located in Guilan province, Iran, a region with an annual rainfall of 1243 mm (average for the last five years). In order to have soil samples with low available phosphate, surface soil samples were selected from the soil adjacent to paddy fields. Samples were air-dried and passed through a 2 mm sieve.

For experiments conducted under anoxic conditions, 1200 g aliquots of the sieved soil samples were placed in plastic buckets (18 cm in diameter) and potable water was gradually added until the height of water reached 8 cm above the soil (details of the water chemistry are

given in Table S1). The samples were mixed manually twice a day for four days until reaching a steady state. Reduced soil subsamples were then removed from the bottom of the buckets (≈ 8-10 cm from the soil surface) with a sampling spoon, 65 to 75 days after submersion.

2.2. Soil physical and chemical characteristics

In air-dried samples, soil pH and soil EC (electrical conductivity) were measured at a 1:5 soil to solution ratio (pH in 0.01 M $CaCl_2$ and EC in deionized water). Soil texture was determined by the hydrometric method (Gee and Bauder 1986). Soil OC was measured by the Walkley-Black method (Allison 1965). Total phosphate was measured by the perchloric acid ($HClO_4$) digestion method (Olsen and Dean 1965). The total concentration of iron oxide phases (such as ferrihydrite, goethite and schwertmannite) was extracted by the DCB (dithionite-citrate-bicarbonate) method (Janitzky 1986). The poorly crystalline iron and aluminum reactive phases (Fe_{ox} and Al_{ox}) were extracted using ammonium oxalate solution, along with the phosphate associated with these phases (Walker 1986). DCB and oxalate extractions were carried out in air-dried soil samples for both oxic and anoxic soils. $PO_{4(ox)}$ was measured only for oxic soils. For the DCB and oxalate extractions, soil samples were passed through a 100-mesh sieve (0.149 mm). The concentration of extracted Fe_{ox} and Al_{ox} was measured by ICP-MS, and the concentration of $PO_{4(ox)}$ by the molybdate blue method using a UV-visible spectrophotometer (Jenway UV/Vis 6505) at a wavelength of 882 nm (Murphy and Riley 1962).

For in-situ measurement of soil pH and soil Eh (redox potential) in the representative soil solution, a plastic tube was placed in the flooded soil within the bucket. Before installation, some small holes were drilled at the bottom end (2 cm from the bottom) of the tube to enable the soil solution to enter the tube. The small holes were covered with a filter paper (MN640) to prevent

150 the entry of soil particles (Fig. 1). Before every measurement, the solution within the tube was
151 removed by a syringe, allowing the fresh soil solution enters the tube from the small holes. Then,
152 pH or Eh electrodes were inserted into the tube. A combined Ag-AgCl electrode was used for pH
153 measurement and a single Pt-Ag and a reference AgCl electrodes (calibrated with ZoBell solution)
154 were used for Eh measurement. The Eh value was recorded when the change in potential was
155 less than 1 mV/min. Dissolved ferrous iron was also measured in the representative soil solution,
156 which was collected with a syringe from the fresh soil solution within the tube, by the 1,10-
157 phenanthroline analytical method (Vogel 1989). The measurements of soil characteristics are
158 presented in Table 1.

159 ## *2.3. Determination of Olsen-P under oxic and anoxic conditions*

160 For oxic soils, the standard Olsen extraction method (Olsen and Dean 1965) was used to
161 determine soil extractable P. Briefly, 100 mL of 0.5 M sodium bicarbonate (buffered at pH=8.5)
162 was added to 5 g of air-dried soil within a 250 ml Erlenmeyer flasks. The suspensions were then
163 shaken for 30 min on an orbital shaker at 200 rpm to prevent soil particles abrasion that could
164 alter the amount of phosphate extracted. After that, they were centrifuged at 2500 rpm for 10
165 min and passed through filter paper (MN640). The experiments were conducted in duplicate. The
166 concentration of phosphate in the filtered solutions was measured by the molybdate blue
167 method using a UV-visible spectrophotometer (Jenway UV/Vis 6505) at 882 nm wavelength
168 (Murphy and Riley 1962).

169 Pre-washed activated carbon was added to the suspensions (0.2 g per 1 g of soil) before
170 shaking, to prevent natural organic matter from competing with phosphate for the binding sites
171 on the soil mineral surfaces. Commercial activated carbon contains a substantial amount of

phosphate; it was therefore washed several times with a sodium bicarbonate solution and deionized water before use. In every experiment, a blank sample of the pre-washed activated carbon was prepared to check for any possible contamination.

For anoxic soils, it is recommended to extract P from wet samples rather than from air-dried samples because air-drying alters the amount extracted (Richardson and Reddy 2013). Therefore, to measure extractable P under anoxic conditions, two wet subsamples were taken simultaneously from the bottom of each bucket. One wet subsample (8 to 10 g, depending on the moisture content, to maintain a final SSR of ~1:20) was placed in contact with 100 mL of 0.5 M sodium bicarbonate to extract the phosphate. The phosphate concentration was then determined by the molybdenum blue method, in a similar way as for the oxic samples. At the same time, the other wet soil subsample (1 g) was oven-dried at 105 ^{o}C to measure the moisture content in the sample and allow for post-experimental correction for changes in the concentration of bicarbonate and the SSR.

2.4. Assessment of the factors affecting the Olsen-P extraction under oxic and anoxic conditions

2.4.1. SSR effect

To evaluate the effect of the SSR, the extractable P was measured at soil to solution (0.5 M sodium bicarbonate, buffered at pH=8.5) ratios of 1:5, 1:7.5, 1:10, 1:15, 1:20, 1:30, 1:40, 1:50, 1:100 and 1:200 kg/L. At the beginning of the experiments, 0.2 g pre-washed activated carbon was added per 1 g of soil.

In the classical Olsen method, the solid to solution ratio is 1:20 and the extraction is done in 250 mL Erlenmeyer flask; while in this experiment, different SSRs should be used at the same

194 container. These conditions may affect differently the motion of the particles in the suspensions
195 and consequently the amount of P extracted. Thus, to eliminate the effect of the container,
196 suspensions were shaken for a longer time. This ensures that the amount of phosphate extracted
197 would not be affected by the volume of the container, and the only variable would be the SSR.
198 Preliminary kinetic experiments using 1:20 SSR and 0.5 M $NaHCO_3$ showed that $S_{0.5}$ and $S_{2.9}$ reach
199 equilibrium after 120 min of shaking, while $S_{1.7}$ requires more time. Therefore, for the SSR
200 experiments, the equilibration time was set at 180 min (Fig. S1). The suspensions were then
201 centrifuged and filtered as previously stated. The phosphate concentration in the filtered solution
202 was measured by the molybdenum blue method.

203 ***2.4.2. Effect of sodium bicarbonate concentration***

204 The effect of sodium bicarbonate concentration (0.1, 0.2, 0.35, 0.5, 0.65, 0.8 and 1 M, all
205 buffered at pH=8.5) on extractable P was investigated on soil samples taken from oxic and anoxic
206 conditions. The suspensions (SSR 1:20) were shaken for 30 min, then centrifuged and filtered. In
207 colorimetric measurements, appropriate blank and standard solutions were used for each
208 sodium bicarbonate concentration to eliminate the possible effect of matrix composition on
209 measured phosphate concentration.

210 For the soil samples taken from anoxic conditions (in both considering the effect of SSR
211 and $NaHCO_3$), the moisture content of the wet soil samples, which may dilute the SSR and
212 extractant, was measured and the changes in the concentration of sodium bicarbonate and SSR
213 were corrected accordingly. Briefly, the final concentrations of NaHCO3 and SSR were calculated
214 based on the amount of moisture added, and then the corrected data were used to make the
215 figures and to use for further calculation/modeling.

2.5. Modeling calculations

The phosphate concentration in the soil solution was predicted using the CD-MUSIC model, with ferrihydrite as a proxy for the (hydr)oxides minerals present in the soil samples. As using common methods (e.g. gas (BET) or organic probe-molecules (ethylene glycol monoethyl ether and humic acid)) to determine the reactive surface area (RSA) is not accurate in a complex system like soil, phosphate was selected as a test ion to assess the RSA in soils in equilibrium with $NaHCO_3$ (0.5 M, pH=8.5) (Hiemstra et al. 2010, Mendez et al. 2020a). Based on Eq. 1, the pool of reversibly adsorbed PO_4 (R-PO_4), i.e. a sink of phosphate bound to the surface sites which can be released into the soil solution, was calculated as follows:

$$R - PO_4 = RSA \times \Gamma + SSR^{-1} \times c \qquad \text{Eq. 1}$$

where *RSA* is the reactive surface area (m^2/kg), Γ is the phosphate surface loading on the metal (hydr)oxide in soil (mol/m^2), *SSR* is the solid to solution ratio (kg/L) and c is the concentration of phosphate in solution (mol/L). The CD-MUSIC model estimates the corresponding phosphate surface loading (Γi) for each measured PO_4 concentration (C_i). The values of RSA and R-PO_4 must then be determined iteratively by consecutive CD model simulations such as when the RSME between experimental and predicted phosphate concentration is minimized. Generally, when pseudo-equilibrium is reached and at least two pairs of data (*i*=2) are available for C_i and SSR_i, the surface area can be calculated by Eq. 2 or optimized by the CD-MUSIC model (Mendez et al. 2020a).

$$RSA = \Delta({SSR^{-1}}_i \times c_i)/\Delta\Gamma_i \qquad \text{Eq. 2}$$

where Δ shows the change in the values of the particular parameters with index *i* = 1 and 2.

The affinity constants and charge distribution coefficients of proton, sodium, carbonate and phosphate, which are required to describe ion binding to the mineral surface were taken from (Mendez et al. 2020a) and are shown in Table S2. Two singly (≡$FeOH^{0.5-}$(a), ≡$FeOH^{0.5-}$(b)) and one triply (≡$Fe_3O^{0.5-}$) coordinated surface groups were defined as reactive sites with effective site densities of 3, 2.8 and 1.41 sites/nm^2, respectively. The capacitances of the inner and outer Stern layers were taken from Hiemstra and Zhao (2016) and established at C_1= 1.15 and C_2= 0.9 F/m^2. The reactive surface area (RSA) and the reversibly adsorbed PO_4 (R-PO_4) were the only parameters that were optimized in the modeling, assuming each soil has its own RSA. The RSA was fitted under both oxic and anoxic conditions while R-PO4 values were fitted for oxic conditions and assumed to be unchanged for anoxic conditions (Table 2). All of the parameters were defined in the CD-MUSIC model. The modeling calculations were carried out using ECOSAT (Keizer and Van Riemsdijk 1994) in combination with FIT (Kinniburgh and Tang 1993).

Singly coordinated surface groups (≡$FeOH^{0.5-}$(a), ≡$FeOH^{0.5-}$(b)) were used to define the interactions between phosphate ions and ferrihydrite surface (Hiemstra and Zhao 2016). It was assumed that ≡$FeOH^{0.5-}$(a) can only form mono- and di-protonated monodentate surface complexes with phosphate (Eq. 3 & 4).

$$\equiv FeOH^{0.5-}(a) + 2H^{+}(aq) + PO_4^{3-}(aq) \leftrightarrow \equiv FeO^{(0.5-)+\Delta Z}{}_0\, PO_2(OH)^{\Delta Z}{}_1 + H_2O\ (l) \qquad \text{Eq. 3}$$

$$\equiv FeOH^{0.5-}(a) + 3H^{+}(aq) + PO_4^{3-}(aq) \leftrightarrow \equiv FeO^{(0.5-)+\Delta Z}{}_0\, PO(OH)_2{}^{\Delta Z}{}_1 + H_2O\ (l) \qquad \text{Eq. 4}$$

while ≡$FeOH^{0.5-}$(b) can form both mono- and di-protonated monodentate and also non-protonated and protonated bidentate phosphate complexes (Eq. 5 - 8).

$$\equiv FeOH^{0.5-}(b) + 2H^{+}(aq) + PO_4^{3-}(aq) \leftrightarrow \equiv FeO^{(0.5-)+\Delta Z}{}_0\, PO_2(OH)^{\Delta Z}{}_1 + H_2O\ (l) \quad \text{Eq. 5}$$

$$\equiv FeOH^{0.5-}(b) + 3H^{+}(aq) + PO_4^{3-}(aq) \leftrightarrow \equiv FeO^{(0.5-)+\Delta Z}{}_0\, PO(OH)_2{}^{\Delta Z}{}_1 + H_2O\ (l) \quad \text{Eq. 6}$$

$$2\equiv FeOH^{0.5-}(b) + 2H^{+}(aq) + PO_4^{3-}(aq) \leftrightarrow \equiv Fe_2\, O_2{}^{(1-)+\Delta Z}{}_0\, PO_2{}^{\Delta Z}{}_1 + 2H_2O\ (l) \quad \text{Eq. 7}$$

$$2\equiv FeOH^{0.5-}(b) + 3H^{+}(aq) + PO_4^{3-}(aq) \leftrightarrow \equiv Fe_2\, O_2{}^{(1-)+\Delta Z}{}_0\, POOH^{\Delta Z}{}_1 + 2H_2O\ (l) \quad \text{Eq. 8}$$

To formulate the interaction between carbonate ion and the mineral surface, carbonate was assumed to form a bidentate surface complex with the ≡$FeOH^{0.5-}$(b) surface group (Eq. 9). This surface complex can also interact with Na^{+} at high sodium concentrations (Eq. 10):

$$2\equiv FeOH^{0.5-}(b) + 2H^{+}(aq) + CO_3^{2-}(aq) \leftrightarrow \equiv Fe_2\, O_2{}^{(1-)+\Delta Z}{}_0\, CO^{\Delta Z}{}_1 + 2H_2O\ (l) \quad \text{Eq. 9}$$

$$2\equiv FeOH^{0.5-}(b) + 2H^{+}(aq) + CO_3^{2-}(aq) + Na^{+}(aq) \leftrightarrow \equiv Fe_2\, O_2{}^{(1-)+\Delta Z}{}_0\, CO\text{-}Na^{\Delta Z}{}_1 + 2H_2O\ (l) \quad \text{Eq. 10}$$

In addition, carbonate may form outer sphere surface complexes with ≡$FeOH^{0.5-}$(a) and ≡$FeOH^{0.5-}$(b) surface groups (Eqs. 11 and 12), but no evidence has been found for the formation of HCO_3^{-} outer sphere complex (Hiemstra and Zhao 2016, Mendez and Hiemstra 2019):

$$\equiv FeOH^{0.5-}(a) + H^{+}(aq) + CO_3^{2-}(aq) \leftrightarrow \equiv FeO^{0.5+\Delta Z}{}_0 \ldots. CO_2{}^{\Delta Z}{}_1 + 1H_2O\ (l) \quad \text{Eq. 11}$$

$$\equiv FeOH^{0.5-}(b) + H^{+}(aq) + CO_3^{2-}(aq) \leftrightarrow \equiv FeO^{0.5+\Delta Z}{}_0 \ldots. CO_2{}^{\Delta Z}{}_1 + 1H_2O\ (l) \quad \text{Eq. 12}$$

It is noted that in the current study, the pH of the sodium bicarbonate extractant solution was set at 8.5. At this pH, organic matter is released into the solution due to the repulsive forces between organic matter and negatively charged surface groups. The released molecules can then be removed by the adsorption on activated carbon. Also, calcium ion in equilibrium with $CaCO_3$(s)

277 may interact with the surface groups (similarly to the magnesium ion). Thus, these interactions
278 were also considered; however, their effects were not significant. Therefore, in the final modeling
279 scenario, the interactions between the mineral surface and organic carbon, calcium and
280 magnesium were not considered.

281 3. Results and discussion

282 *3.1. Soil physical and chemical characteristics*

283 The pH of soil samples $S_{0.5}$ and $S_{2.9}$ were acidic and $S_{1.7}$ was almost neutral. The soils had
284 a very low EC and the OC contents were 0.54, 1.72, and 2.87% for $S_{0.5}$, $S_{1.7}$ and $S_{2.9}$ samples,
285 respectively. Soil texture was clayey for $S_{0.5}$ and $S_{2.9}$ and silty clay for $S_{1.7}$. The amount of Fe_{DCB}
286 ranged from 172 to 460 mmol/kg, and the Fe_{OX} from 32 to 135 mmol/kg, i.e. 20-30% of total iron
287 oxides were present in the form of poorly crystalline phases. By contrast, the amount of Al_{OX} was
288 very similar in all three samples, ranging between 66 and 78 mmol/kg. The amount of oxalate-P
289 in the soil samples was very high (1.31 to 20.60 mmol/kg), relative to the amount of Olsen-P (i.e.
290 the extractable fraction) (0.06 to 0.21 mmol/kg). Similarly, the Olsen-P represented less than 1%
291 of the total phosphate (Table 1). The average amount of Olsen-P, pH and OC in agricultural paddy
292 lands in the region where the samples were collected are approximately 0.39 mmol/kg, 7 and
293 2%, respectively (Davatgar et al. 2015).

294 During the flooding experiment, the pH and Eh values of the soil samples were monitored
295 periodically until day 65, when both variables reached a steady state. The pH values in samples
296 $S_{0.5}$ and $S_{2.9}$, which were initially acidic, increased to nearly neutral values, while in sample $S_{1.7}$,
297 which was initially almost neutral, did not vary significantly (Fig. 2a). The Eh value in all samples

298 decreased with the flooding time, indicating a change from oxic to anoxic conditions. The final Eh
299 values were approximately +160, -60, and -75 mV in samples $S_{0.5}$, $S_{1.7}$, and $S_{2.9}$, respectively (Fig.
300 2b). The lower Eh values in $S_{1.7}$ and $S_{2.9}$ are possibly due to the higher OC content in these samples
301 (Fageria et al. 2011). The correlation between delta Eh and %OC in samples $S_{0.5}$, $S_{1.7}$, and $S_{2.9}$ is
302 shown in Fig. S2. This figure shows that the difference between the initial and final Eh values
303 increased with the amount of OC in the soil samples. After day 65, the soil samples can be
304 considered anoxic, although the Eh of sample $S_{0.5}$ ranged between suboxic and anoxic.

305 The differences in the amount of crystalline iron (Fe_{crysl}, calculated by subtracting Fe_{ox}
306 from Fe_{DCB}) and poorly crystalline iron, Fe_{ox}, were measured in the submerged samples. The
307 relative content of Fe_{crysl} (Fig. 3a) indicates that as the flooding time increases, the amount of
308 Fe_{crysl} decreases in sample $S_{2.9}$, while it barely changes in samples $S_{0.5}$ and $S_{1.7}$. The variation in the
309 poorly crystalline iron with flooding time is consistent with these results, i.e. the amount of Fe_{ox}
310 increases for the $S_{2.9}$, while no variation is found for samples $S_{1.7}$ and $S_{0.5}$ (Fig. 3b). This change
311 can be attributed to the reductive dissolution of iron minerals into the soil solution in sample $S_{2.9}$.
312 In addition, in another two samples a sharp release of ferrous iron into the solution as a result of
313 reductive dissolution is observed (Fig. 4). The significant increase in ferrous iron concentration in
314 the samples specifically occurred in the first few weeks (20 days) after the flooding. The amounts
315 of ferrous iron in the first measurement in the solutions (5 days after flooding) were 0.25, 2.8 and
316 67 µmol/L and reached 80, 55 and 650 µmol/L (measurement on day 20) for samples $S_{0.5}$, $S_{1.7}$ and
317 $S_{2.9}$ respectively. As the amount of dissolved iron in the solution was very low relative to the
318 amount of iron in the solid phase, a small change in the Eh values can lead to a marked change

in ferrous iron in the solution. Therefore, the trends in the solid phases are not as clear as for iron in the solution.

3.2 Desorption experiments

3.2.1 Effect of SSR under oxic and anoxic conditions

Under oxic conditions, the concentration of extracted P in the solution increases with the SSR (Fig. 5a), which is consistent with previous findings (Barrow and Shaw 1976a, Hiemstra et al. 2010). The initial amount of phosphate was higher in sample $S_{1.7}$ than in the other samples. Thus, the difference in extracted P among the soil samples can be attributed to the phosphate loading. As can be seen in Fig. 5a, at low SSR (1:100 and 1:200), due to the increase in the total amount of bicarbonate ions, the competitive bicarbonate-phosphate interaction and also the soil dilution condition led to the release of a larger fraction of the initially adsorbed phosphate. As the SSR increases gradually, the fraction of released phosphate from the reactive sites decreases. As such, at higher SSR, phosphate is mainly released from the external surfaces of mineral oxide aggregates (iron and aluminum (hydr)oxides) and edges of clay minerals, whereas at lower SSR, in addition to the external surfaces, phosphate is also slowly released from the internal aggregate surfaces (Hiemstra et al. 2010). The effect of the SSR on the extraction of phosphate from soil has generally been attributed to different factors, including the presence of colloids, interactions between particles, kinetic effects and heterogeneity (Lucero et al. 1998).

In the present study, we observed that the concentration of phosphate released at low SSR is 3 to 7 times lower than that extracted by the standard Olsen method (Table 1), and the relationship was non-linear. In samples $S_{0.5}$ and $S_{2.9}$, the variation in the concentration of extracted phosphate was low (i.e. high phosphate buffering). This may be associated with a larger

reactive surface area in the soil samples (Table 2). A high iron (hydr)oxide content may also result in a lower effect of SSR on the extractable P. The variation in extracted P as a function of SSR is greater in sample $S_{1.7}$ than in the other samples, possibly as a result of higher initial Olsen-P and lower content of iron (hydr)oxides. On the other hand, the initial pH value of this sample is higher than 7. Under these conditions, dissolved Ca precipitates as $CaCO_3$(s) and promotes the dissolution of calcium phosphate (Braun et al. 2019). The slight slope in sample $S_{2.9}$ can be attributed to the lower amount of extractable P than in sample $S_{1.7}$, while in sample $S_{0.5}$ it can be attributed to both the lower amount of extractable P and the lower OC content. Mendez et al. (2020a) also observed different trends in soil samples due to the different buffering capacities (Fig. S3).

The effect of SSR in the anoxic condition was also investigated and the results are also shown in Fig 5a. Similar to the oxic conditions, the phosphate released into the solution under anoxic conditions increases with SSR. In sample $S_{0.5}$, changing the SSR and Eh had a weak effect on the extractable P. This sample contains low OC and high iron (hydr)oxides (Table 1); thus, there is less competition for the reactive sites on iron (hydr)oxides, and the phosphate buffering capacity is high. The relatively high Eh value, +160 mV, also greatly reduces the effect of changing from oxic to anoxic conditions on the extracted phosphate for this sample (Figs. 5a and S4a). On the other hand, for samples $S_{1.7}$ and $S_{2.9}$ the effect of SSR is higher under anoxic conditions than under oxic conditions (Figs. 5a, S4b and S4c). For sample $S_{2.9}$ this effect was higher at low SSR values (Figs. 5a and S4c). Under anoxic conditions, due to the lower redox potential in the soil system, reductive dissolution of iron (hydr)oxides surface may be occurring, resulting in the release of adsorbed phosphate (Hanke et al. 2014).

3.2.2 The effect of sodium bicarbonate concentration under oxic and anoxic conditions

The results show that more phosphate is released to the solution phase as the concentration of sodium bicarbonate increases (Fig. 5b), which can be attributed to competition between bicarbonate and phosphate for the reactive sites on the soil mineral oxides (Rahnemaie et al. 2007a, Hiemstra et al. 2010, Mendez and Hiemstra 2019). In sample $S_{0.5}$, the amount of phosphate released into the solution do not vary significantly upon increasing the concentration of $NaHCO_3$. Because of the low OC content and relatively high content of iron (hydr)oxides in this sample, a high level of phosphate buffering is expected. The same is observed for sample $S_{2.9}$, which contains greater amounts of poorly crystalline and crystalline iron (hydr)oxides (Table 1). If the specific surface area is relatively large, the mineral surface will have enough reactive sites available for both phosphate and bicarbonate ions to be adsorbed (Yan et al. 2016). The variation in phosphate as a function of bicarbonate concentration in sample $S_{1.7}$ is greater than in the other samples, possibly due to the low content of iron (hydr)oxides.

Changes in the extracted phosphate as a function of sodium bicarbonate concentration have been reported to be more marked at lower concentrations of sodium bicarbonate (<0.5 M) (Hiemstra et al. 2010), which was not observed in the current study. The difference in findings is probably due to the fact that in the present study the soil samples relatively contain lower concentration of phosphate than their arable topsoils. Different slopes indicate that phosphate may be bound to the sites with different surface adsorption energies. Therefore, by increasing the bicarbonate concentration, the phosphate bound to the low energy sites is released first and the ability of bicarbonate ions to outcompete and release phosphate bound to the high energy sites gradually decreases. In the present study, the change in the concentration of extracted

phosphate as a function of the bicarbonate concentration is linear for all three samples. When the concentration of phosphate is low, as in the case of these soil samples, high-energy sites are preferred. By increasing the concentration of bicarbonate, the phosphate bound to the high-energy surface groups will be gradually released. The increase in the concentration of the extracted phosphate with the bicarbonate concentration is due to the decrease in the re-adsorption process (Barrow and Shaw 1976b).

The effect of sodium bicarbonate concentration on extractable P in the anoxic samples is also presented in Fig. 5b. Similar to the oxic samples, for the flooded soils a positive and linear relationship between the extracted phosphate and the concentration of bicarbonate was observed. However, for sample $S_{0.5}$ the increase was less pronounced than for samples $S_{1.7}$ and $S_{2.9}$, which may indicate the higher phosphate buffering capacity of this soil sample. As stated above, the phosphate-bicarbonate competition for the reactive sites at the soil mineral surfaces is the cause of the increase in the extracted phosphate with the sodium bicarbonate concentration (Mendez and Hiemstra 2019).

The phosphate extracted from sample $S_{0.5}$ collected from the flooded buckets was not remarkably different from that observed under oxic conditions. In this sample, the Eh value was relatively high, +160 mV, i.e. suboxic conditions, and the initially measured extractable P was lower than for the other samples. Because the ferric iron is not considered an electron acceptor at redox potentials above +150 mV (Amini et al. 2020), changing from oxic to suboxic conditions has only a small effect on the amount of extracted phosphate. On the other hand, for samples $S_{1.7}$ and $S_{2.9}$, the effect of bicarbonate concentration on the release of phosphate was greater under anoxic conditions than under oxic conditions. Due to the competition between

bicarbonate and phosphate, more phosphate is released as the concentration of HCO_3^- increases. The competition is more pronounced under anoxic conditions, possibly due to the lower Eh values in the systems. When the Eh value is relatively low, ferrous iron is released into the solution by reductive dissolution of the iron oxide minerals, and the phosphate bound to these surfaces will be readily released into the solution (Gu et al. 2019). The presence of bicarbonate ions prevents re-adsorption of the released phosphate onto the surfaces.

3.3. Modeling calculations

3.3.1. SSR

The CD-MUSIC model reasonably described the experimental data and the effect of varying the SSR for all samples, under both oxic and anoxic conditions, as observed when the predictions and the experimental data are correlated (Fig. 6). The parameters fitted to the SSR data were used to simulate the effect of change in the bicarbonate concentration on the extractable P (see supplementary material, Fig. S5). As stated above, the only parameters fitted were the RSA and R-PO_4 (Table 2); the surface complexation constants were taken from previous studies (Table S2). The fitted values for the R-PO_4 were lower than the measured oxalate-extractable phosphate (Table 1). The difference between measured oxalate-P and fitted R-PO_4 is possibly due to a low initial amount of oxalate-P in the samples. Low initial oxalate-P values can lead to an error in the measurements. Oxalate can dissolve Fe and Al simultaneously, leading to a greater release of phosphate from the soil matrix and overestimation of the values (Hiemstra et al. 2010). On the other hand, oxalate-P was measured in the finer fraction of soil samples (0.149 mm sieve), while the fitted values are based on the phosphate extracted in <2 mm sized particles. When soil samples are passed through a finer sieve, the portion of iron oxides to the

429 weight of the soil sample will increase. In this case, greater amounts of P will be released into the
430 solution as oxalate-P is bound to the mineral oxides.

431 The fitted RSA values for $S_{0.5}$, $S_{1.7}$ and $S_{2.9}$ samples were 7.50, 1.62 and 8.37 m^2/g,
432 respectively. Considering oxalate extractable iron and aluminum, the RSA values were converted
433 to the specific surface area (SSA) values of the (hydr)oxide minerals, which were 560, 176 and
434 445 m^2/g (hydr)oxide. Except for sample $S_{1.7}$, the values were approximately in the range of SSA
435 obtained in the study of Mendez et al. (2020a) for agricultural soils, which ranged between 347
436 and 1406 m^2/g oxide. The SSA values were calculated from RSA, using oxalate extractable
437 fraction of Fe and Al and assuming the molar mass of 97 g/mol Fe (ferrihydrite) and 78 g/mol Al
438 (gibbsite) (Hiemstra et al. 2010). The oxalate-extractable fraction of Fe was measured under both
439 oxic and anoxic conditions, and therefore different values of Fe_{ox} were used to calculate SSA
440 under these conditions. On the other hand, as Al oxides are not reduced at the measured Eh
441 values of all soil samples and the measured values of Al_{ox} in anoxic samples were not significantly
442 different from those measured under oxic conditions, Al_{ox} was therefore assumed constant for
443 SSA calculations under both oxic and anoxic conditions.

444 Under anoxic conditions, the modeling parameters were initially set to those obtained
445 under oxic conditions, but the model underestimated the phosphate concentration in the
446 solution. The surface complexes of ferrous iron with the surface groups of ferrihydrite and
447 ternary surface complexes of ferrous iron and phosphate with the surface sites were then
448 considered in the modeling approach, as proposed by (Talebi Atouei (2016)), to consider possible
449 re-adsorption of Fe and implications of this re-adsorption on the surface charge of the mineral
450 that promotes P adsorption. The concentration of ferrous iron, which was defined as a model

component, was measured in the flooded soils (6<pH<7) and thus included in the model simulations. Nevertheless, even with the inclusion of ferrous iron, the model underestimated the experimentally measured data. This is possibly due to the pH (buffered to 8.5) of the soil samples for the bicarbonate extraction. The presence of carbonate in the soil solution and the low value of Eh can limit the solubility of ferrous iron because of the effect of carbonates on the pH of the solution and the low solubility of ferrous carbonate in case of its formation (Hem 1960).

As previously stated, under anoxic conditions, the reductive dissolution of iron (hydr)oxide minerals may occur, and additional ferrous iron may then be released into the solution (Herndon et al. 2020). The dissolved ferrous iron can diffuse to the oxic layer, where it is easily oxidized and reprecipitated as poorly crystalline iron minerals (Tian et al. 2017). Both processes may affect the RSA. By defining surface complexes similar to those formed under oxic conditions and additional fitting of the surface area, the CD-MUSIC model can describe experimental data under anoxic conditions (Fig. 6 and Fig. S4). The fitted values for RSA and also calculated values of SSA were lower than those obtained for oxic conditions. The differences between the fitted values for the RSA under oxic and anoxic conditions for $S_{0.5}$, $S_{1.7}$, and $S_{2.9}$ samples were 26, 47 and 27 % respectively (Table 2). Although new iron minerals may be formed in sample $S_{2.9}$, a net decrease in SSA, from 445 to 195 m^2/g, was observed; this was not expected, based on the information in Fig. 3b. The decrease in SSA for samples $S_{0.5}$ and $S_{1.7}$ may be attributed to the reductive dissolution of Fe mineral phases, which cause preferential dissolution of mineral phases with higher SSA and larger solubility, leaving only the more stable Fe oxide minerals remaining in the solid phases (Fig. 3a & 4).

3.3.2. Bicarbonate

To describe the effect of change in the bicarbonate concentration on the extractable phosphate, all the model parameters previously defined (section 3.3.1), including the RSA and R-PO_4, were used. Model predictions versus experimental observations were also shown in Fig S5. By using the same RSA and reactive phosphate pool as for the SSR experiments (i.e. under oxic conditions), the model could describe the experimental data reasonably well, although it overestimates the extractable phosphate in sample $S_{1.7}$. This overestimation is most likely caused by the lower equilibration time in the sodium bicarbonate experiments (30 min) compared to the SSR experiments (180 min). As stated before, in the initial kinetic experiments (Fig. S1), data showed that samples $S_{0.5}$ and $S_{2.9}$ reached a pseudo-equilibrium within 30 min of shaking, but sample $S_{1.7}$ did not. On the other hand, a low initial phosphate concentration may result in a larger error in the measurements, which may lead to a larger difference between the model output and the experimental data.

The parameters obtained in the modeling of the SSR experimental data under anoxic conditions were also used to predict the effect of the bicarbonate-phosphate competition. The modeling predictions were well correlated with the experimental observations, although we observed some deviations at high bicarbonate concentration for sample $S_{1.7}$. Sensitivity calculations were conducted to assess the effect of changing the Stern capacitance or considering the presence of ferrous iron and organic matter on the model predictions, but the predictions did not change significantly. Nevertheless, it seems that the predictions for the anoxic samples are better than for the oxic samples, with less deviations between experimental observations and modeling predictions for the former. The amount of extractable phosphate increased in

comparison to that obtained under oxic conditions, reducing the possibility of errors in the measurements.

4. Conclusions

The effects of SSR (solid to solution ratio) and bicarbonate concentration on phosphate extractability under oxic and anoxic conditions were compared. By increasing the SSR and bicarbonate concentration, the concentration of phosphate in the solution was increased. The findings indicate that low Eh values intensify the effect of SSR and $NaHCO_3$ concentration on phosphate extractability, possibly due to the reductive dissolution of iron oxide minerals. The differences between oxic and anoxic conditions are variable and depend on the Eh value, the amount of iron (hydr)oxides and the phosphate buffering capacity.

The extractable P in the soil solution was simulated by the well parametrized CD-MUSIC model, allowing the RSA (reactive surface area) of the soil samples to be determined under both oxic and anoxic conditions. The SSA (specific surface area) of the soil samples decreased when anoxic conditions were established after flooding, possibly due to the reductive dissolution of iron (hydr)oxides and the formation of new solid phases with lower reactive surface area. The findings also demonstrate that, although an increase in soil SSA decreases phosphate extractability under both oxic and anoxic conditions, the effect is three times greater under anoxic conditions.

Overall, our experimental data and model outputs shed further light on the complicated chemistry of phosphate extractability in flooded soils and other soil samples under anoxic

conditions. However, for a more general and universal picture, the present findings can be used in the future to better understand the effect of different variables in soil samples.

Acknowledgments

The authors thank the research council of the Tarbiat Modares University for the financial support and laboratory assistance received by Mrs. Tabibzadeh and Dr. Abdollahpour. The authors are also grateful for financial support provided by Xunta de Galicia - Consellería de Educación e Ordenación Universitaria de Galicia (Consolidation of Competitive Groups of Investigation; GI-1245, ED431C 2018/12) and by CRETUS Strategic Group (AGRUP2015/02).

References

Allison, L. E. 1965. Organic Carbon. Methods of Soil Analysis. Part 2. Chemical and Microbiological Properties. American Society of Agronomy, Soil Science Society of America.

Amini, M., J. Antelo, S. Fiol, and R. Rahnemaie. 2020. Modeling the effects of humic acid and anoxic condition on phosphate adsorption onto goethite. Chemosphere **253**:126691.

Antelo, J., S. Fiol, C. Pérez, S. Mariño, F. Arce, D. Gondar, and R. López. 2010. Analysis of phosphate adsorption onto ferrihydrite using the CD-MUSIC model. Journal of Colloid and Interface Science **347**:112-119.

Barrow, N. J., and T. C. Shaw. 1976a. Sodium bicarbonate as an extractant for soil phosphate, I. Separation of the factors affecting the amount of phosphate displaced from soil from those affecting secondary adsorption. Geoderma **16**:91-107.

Barrow, N. J., and T. C. Shaw. 1976b. Sodium bicarbonate as an extractant for soil phosphate, II. Effect of varying the conditions of extraction on the amount of phosphate initially displaced and on the secondary adsorption. Geoderma **16**:109-123.

Braun, S., R. Warrinnier, G. Börjesson, B. Ulén, E. Smolders, and J. P. Gustafsson. 2019. Assessing the ability of soil tests to estimate labile phosphorus in agricultural soils: Evidence from isotopic exchange. Geoderma **337**:350-358.

Cosmidis, J., K. Benzerara, G. Morin, V. Busigny, O. Lebeau, D. Jézéquel, V. Noël, G. Dublet, and G. Othmane. 2014. Biomineralization of iron-phosphates in the water column of Lake Pavin (Massif Central, France). Geochimica et Cosmochimica Acta **126**:78-96.

Davatgar, N., A. Zare, M. Shakoori Katigari, L. Rezaei, M. Kavousi, H. Shaykh al-Islam, M. Shahnazari, E. Kohneh, A. Shirinfekr, I. Bonyadi, S. Adibi, I. Moshirtalesh, A. Khodashenas, H. Shokri Vahed, F. Dori, S. A. Rahimi Moghadam, and A. Ajili Lahiji. 2015. Investigation of fertility status of paddy soils in Guilan province. Journal of Land management **3**:1-13.

547 Devau, N., E. L. Cadre, P. Hinsinger, B. Jaillard, and F. Gérard. 2009. Soil pH controls the environmental
548 availability of phosphorus: Experimental and mechanistic modelling approaches. Applied
549 Geochemistry **24**:2163-2174.
550 Fageria, N., G. Carvalho, A. Santos, E. Ferreira, and A. Knupp. 2011. Chemistry of lowland rice soils and
551 nutrient availability. Communications in Soil Science and Plant Analysis **42**:1913-1933.
552 Gee, G. W., and J. W. Bauder. 1986. Particle-size Analysis. Methods of Soil Analysis: Part 1—Physical and
553 Mineralogical Methods.
554 Groenenberg, J. E., P. F. A. M. Römkens, A. V. Zomeren, S. M. Rodrigues, and R. N. J. Comans. 2017.
555 Evaluation of the single dilute (0.43 M) nitric acid extraction to determine geochemically reactive
556 elements in soil. Environmental Science & Technology **51**:2246-2253.
557 Gu, S., G. Gruau, R. Dupas, P. Petitjean, Q. Li, and G. Pinay. 2019. Respective roles of Fe-oxyhydroxide
558 dissolution, pH changes and sediment inputs in dissolved phosphorus release from wetland soils
559 under anoxic conditions. Geoderma **338**:365-374.
560 Gustafsson, J. P. 2001. Modelling competitive anion adsorption on oxide minerals and an allophane-
561 containing soil. European Journal of Soil Science **52**:639-653.
562 Hanke, A., M. Sauerwein, K. Kaiser, and K. Kalbitz. 2014. Does anoxic processing of dissolved organic
563 matter affect organic–mineral interactions in paddy soils? Geoderma **228–229**:62-66.
564 Hem, J. D. 1960. Restraints on dissolved ferrous iron imposed by bicarbonate redox potential, and pH. US
565 Government Printing Office.
566 Herndon, E., L. Kinsman-Costello, N. Di Domenico, K. Duroe, M. Barczok, C. Smith, and S. D. Wullschleger.
567 2020. Iron and iron-bound phosphate accumulate in surface soils of ice-wedge polygons in arctic
568 tundra. Environmental Science: Processes & Impacts **22**:1475-1490.
569 Hiemstra, T., J. Antelo, R. Rahnemaie, and W. H. v. Riemsdijk. 2010. Nanoparticles in natural systems I:
570 The effective reactive surface area of the natural oxide fraction in field samples. Geochimica et
571 Cosmochimica Acta **74**:41-58.
572 Hiemstra, T., S. Mia, P.-B. Duhaut, and B. Molleman. 2013. Natural and Pyrogenic Humic Acids at Goethite
573 and Natural Oxide Surfaces Interacting with Phosphate. Environmental Science & Technology
574 **47**:9182-9189.
575 Hiemstra, T., and W. Zhao. 2016. Reactivity of ferrihydrite and ferritin in relation to surface structure, size,
576 and nanoparticle formation studied for phosphate and arsenate. Environmental Science: Nano
577 **3**:1265-1279.
578 Horta, M. d. C., and J. Torrent. 2007. The Olsen P method as an agronomic and environmental test for
579 predicting phosphate release from acid soils. Nutrient Cycling in Agroecosystems **77**:283-292.
580 Janitzky, P. 1986. Field and laboratory procedures used in a soil chronosequence study. Report 1648,
581 Washington, D.C.
582 Keizer, M., and W. Van Riemsdijk. 1994. ECOSAT: equilibrium calculation of speciation and transport,
583 manual program. Agricultural University of Wageningen, Wageningen,the Netherlands.
584 Kinniburgh, D., and C. Tang. 1993. FIT; Technical Report WD/93/23;. British Geological Survey. Natural
585 Environment Research Council, Keyworth, Great Britain.
586 Loeb, R., L. P. M. Lamers, and J. G. M. Roelofs. 2008. Prediction of phosphorus mobilisation in inundated
587 floodplain soils. Environmental Pollution **156**:325-331.
588 Lucero, D. W., D. C. Martens, J. R. McKenna, and D. E. Starner. 1998. Comparison of Mehlich 3- and bray
589 1-extractable phosphorus levels in a Starr clay loam amended with poultry litter. Communications
590 in Soil Science and Plant Analysis **29**:1133-1142.
591 McDowell, R. W., and A. N. Sharpley. 2003. Phosphorus solubility and release kinetics as a function of soil
592 test P concentration. Geoderma **112**:143-154.
593 Mendez, J. C., and T. Hiemstra. 2019. Carbonate Adsorption to Ferrihydrite: Competitive Interaction with
594 Phosphate for Use in Soil Systems. ACS Earth and Space Chemistry **3**:129-141.

595 Mendez, J. C., and T. Hiemstra. 2020b. Surface area of ferrihydrite consistently related to primary surface
596 charge, ion pair formation, and specific ion adsorption. Chemical Geology **532**:119304.
597 Mendez, J. C., T. Hiemstra, and G. F. Koopmans. 2020a. Assessing the reactive surface area of soils with
598 ferrihydrite as proxy for natural oxide nanoparticles. Environmental Science & Technology **209**.
599 Murphy, J., and J. P. Riley. 1962. A modified single solution method for the determination of phosphate in
600 natural waters. Analytica Chimica Acta **27**:31-36.
601 Olsen, S. R., C. W. Cole, F. Watanabe, and L. A. Dean. 1954. Estimation of Available Phosphorus in Soils by
602 Extraction with Sodium Bicarbonate. U.S. Department of Agriculture.
603 Olsen, S. R., and L. A. Dean. 1965. Phosphorus. Methods of Soil Analysis. Part 2. Chemical and
604 Microbiological Properties. American Society of Agronomy, Soil Science Society of America.
605 Pant, H. K., and K. R. Reddy. 2001. Phosphorus Sorption Characteristics of Estuarine Sediments under
606 Different Redox Conditions. Journal of Environmental Quality **30**:1474-1480.
607 Ponnamperuma, F. 1972. The chemistry of submerged soils. Academic Press NY and London.
608 Rahnemaie, R., T. Hiemstra, and W. H. van Riemsdijk. 2007a. Carbonate adsorption on goethite in
609 competition with phosphate. Journal of Colloid and Interface Science **315**:415-425.
610 Rahnemaie, R., T. Hiemstra, and W. H. van Riemsdijk. 2007b. Geometry, charge distribution, and surface
611 speciation of phosphate on goethite. Langmuir **23**:3680-3689.
612 Richardson, C. J., and K. R. Reddy. 2013. Methods for Soil Phosphorus Characterization and Analysis of
613 Wetland Soils. In Methods in Biogeochemistry of Wetlands. In: R. DeLaune, K. R. Reddy, C.
614 Richardson and J. Megonigal (Eds.). Soil Science Society of America:603-638.
615 Saeed, H., A. Hartland, N. J. Lehto, M. Baalousha, M. Sikder, D. Sandwell, M. Mucalo, and D. P. Hamilton.
616 2018. Regulation of phosphorus bioavailability by iron nanoparticles in a monomictic lake.
617 Scientific Reports **8**:17736.
618 Sah, R., D. Mikkelsen, and A. Hafez. 1989. Phosphorus behavior in flooded-drained soils. II. Iron
619 transformation and phosphorus sorption. Soil Science Society of America Journal **53**:1723-1729.
620 Shahandeh, H., L. R. Hossner, and F. T. Turner. 1994. Phosphorus Relationships in Flooded Rice Soils with
621 Low Extractable Phosphorus. Soil Science Society of America Journal **58**.
622 Sibbesen, E. 1983. Phosphate soil tests and their suitability to assess the phosphate status of soil. Journal
623 of the Science of Food and Agriculture **34**:1368-1374.
624 Talebi Atouei, M. 2016. Prediction of the chemical behavior of phosphorus in paddy soils (Doctoral thesis,
625 Tarbiat Modares University).
626 Tian, J., G. Dong, R. Karthikeyan, L. Li, and R. D. Harmel. 2017. Phosphorus Dynamics in Long-Term Flooded,
627 Drained, and Reflooded Soils. Water **9**:531.
628 Vogel, A. I. 1989. Vogel's Textbook of Quantitative Chemical Analysis. In: G.H. Jeffery, J. Bassett, J.
629 Mendham and R.C. Denney (Eds.). 5th Edition. Longman Scientific and Technical, Harlow.:690-
630 691.
631 Walker, A. 1986. Field and laboratory procedures used in a soil chronosequence study. Report 1648,
632 Washington, D.C.
633 Weng, L., W. H. Van Riemsdijk, and T. Hiemstra. 2008. Humic Nanoparticles at the Oxide−Water Interface:
634 Interactions with Phosphate Ion Adsorption. Environmental Science & Technology **42**:8747-8752.
635 Weng, L., W. H. Van Riemsdijk, and T. Hiemstra. 2012. Factors controlling phosphate interaction with iron
636 oxides. Journal of Environmental Quality **41**:628-635.
637 Weng, L., F. A. Vega, and W. H. Van Riemsdijk. 2011. Competitive and Synergistic Effects in pH Dependent
638 Phosphate Adsorption in Soils: LCD Modeling. Environmental Science & Technology **45**:8420-
639 8428.
640 Wuenscher, R., H. Unterfrauner, R. Peticzka, and F. Zehetner. 2015. A comparison of 14 soil phosphorus
641 extraction methods applied to 50 agricultural soils from Central Europe. Plant, Soil and
642 Environment **61**:86-96.

643 Yan, J., T. Jiang, Y. Yao, S. Lu, Q. Wang, and S. Wei. 2016. Preliminary investigation of phosphorus
644 adsorption onto two types of iron oxide-organic matter complexes. Journal of Environmental
645 Sciences **42**:152-162.
646 Zhang, Y., X. Lin, and W. Werner. 2003. The effect of soil flooding on the transformation of Fe oxides and
647 the adsorption/desorption behavior of phosphate. Journal of Plant Nutrition and Soil Science
648 **166**:68-75.

649

650

651 **Table 1.** Physical and chemical characteristics of $S_{0.5}$, $S_{1.7}$ and $S_{2.9}$ soil samples

Soil	pH*	EC**	OC	Clay	Fe_{ox}***	Al_{ox}***	$PO_{4(ox)}$***	Fe_{DCB}***	$[PO_4]_T$	$[PO_4]_{Olsen}$ (Oxic)	$[PO_4]_{Olsen}$ (Anoxic)	$[Fe^{2+}]$**** (Anoxic)
		dS/m	------ % ------		---------- mmol/kg ----------							µM
($S_{0.5}$)	4.80	0.07	0.54	41	84	67	1.31	329	22	0.063	0.069	163.7
($S_{1.7}$)	7.15	0.08	1.72	44	32	78	20.60	172	45	0.213	0.442	45.3
($S_{2.9}$)	5.20	0.10	2.87	42	134	74	2.50	457	23	0.176	0.187	265.8

652 * Soil pH was measured in 1:5 soil to solution (0.01 M $CaCl_2$) ratio under oxic conditions

653 ** Soil EC was measured in 1:5 soil to solution (deionized water) ratio under oxic conditions

654 *** For measuring these parameters under oxic conditions, soil samples were passed through a 0.149 mm sieve; ox stands for
655 oxalate and DCB for Dithionite-Citrate-Bicarbonate

656 **** Ferrous iron was measured in representative soil solutions taken from flooded soils in buckets under anoxic conditions

657

658

659

660

661

662

663

664

665

Table 2. Fitted reactive surface area (RSA) and reversibly adsorbed phosphate (R-PO_4) by the CD-MUSIC model for $S_{0.5}$, $S_{1.7}$ and $S_{2.9}$ soil samples used to describe the effect of SSR on extracted P

Soil	R-PO_4* mmol/kg	RSA** m^2/g soil	SSA*** m^2/g oxide	R-PO_4* mmol/kg	RSA** m^2/g soil	SSA*** m^2/g oxide
	Oxic			Anoxic		
($S_{0.5}$)	0.31	7.50	560	0.31	5.56	363
($S_{1.7}$)	0.58	1.62	176	0.58	0.85	74
($S_{2.9}$)	0.80	8.37	445	0.80	6.11	195

* Fitted reversibly adsorbed phosphate. R-PO_4 values were assumed to be the same for oxic and anoxic conditions

** Fitted reactive surface area, RSA fitted under both oxic and anoxic conditions

*** Specific surface area, SSA values were calculated, according to the method described in the text, from RSA values

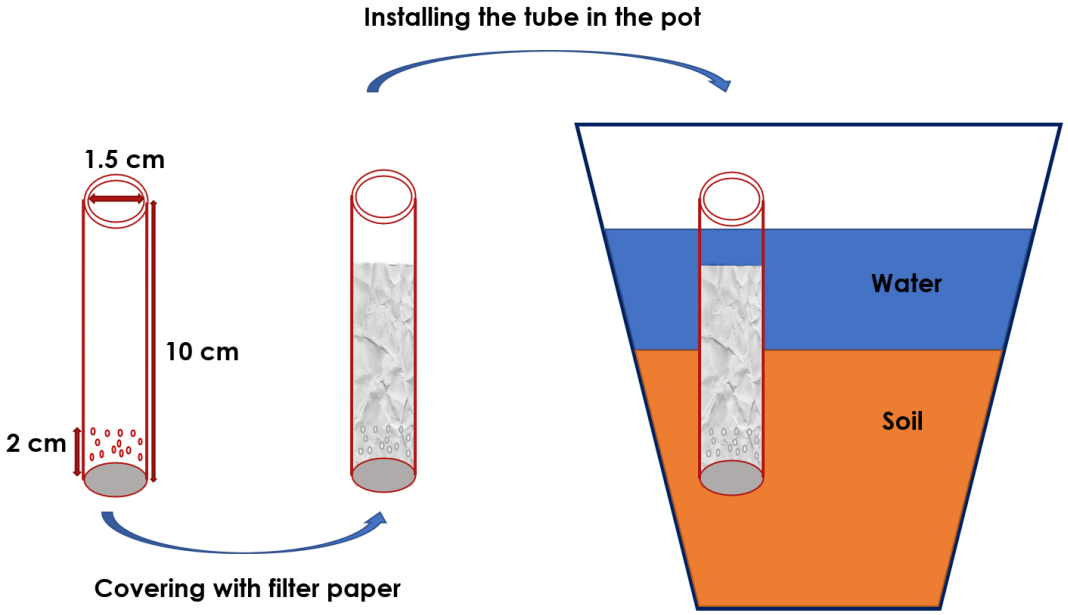

Fig.1. Schematic figure of installed tube covered with filter paper in flooded pots for pH, Eh and Fe (II) measurements

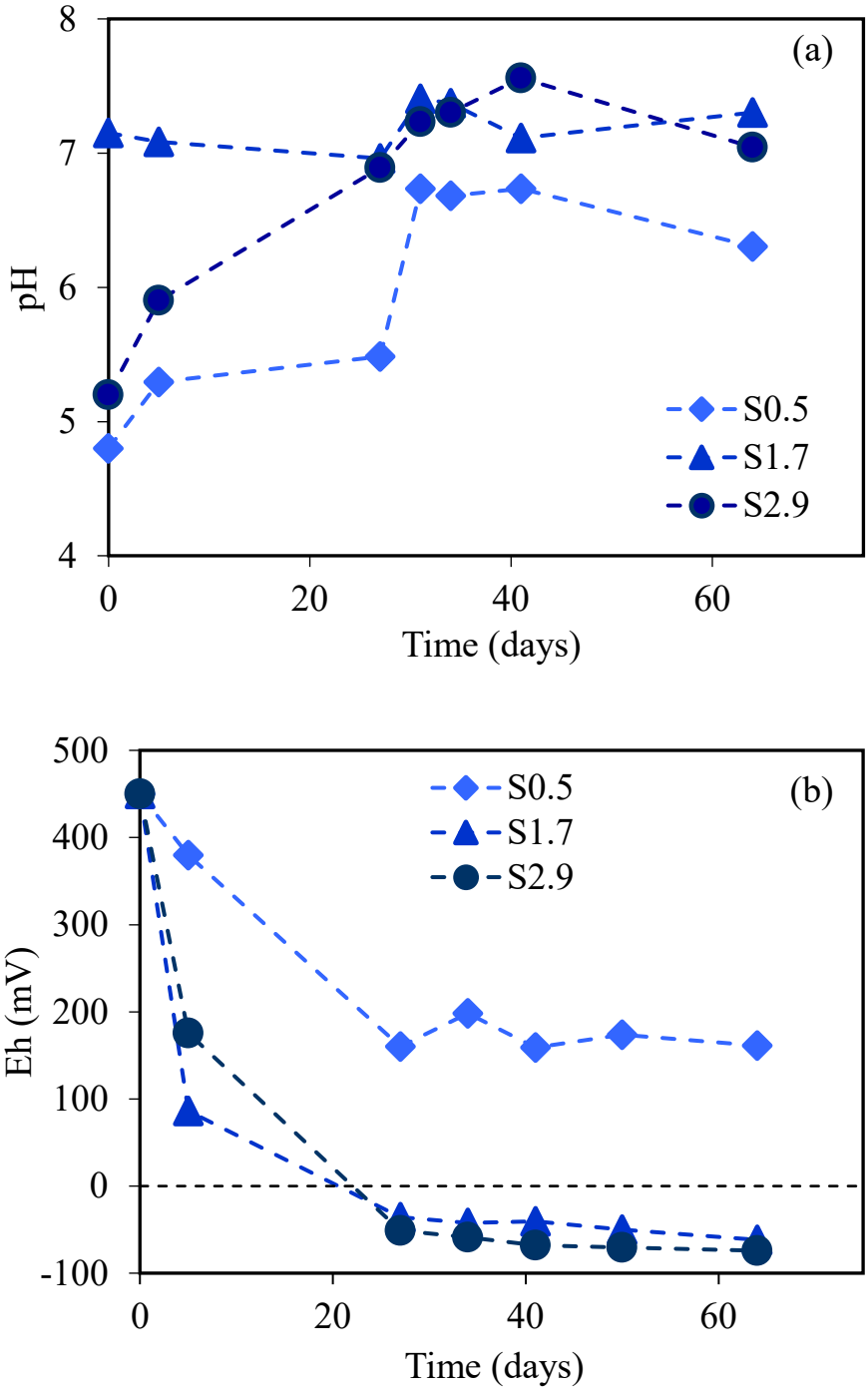

680
681
682
683 **Fig.2.** Effect of flooding time (days) on a) pH and b) Eh (mV) in $S_{0.5}$, $S_{1.7}$ and $S_{2.9}$ soil samples.

684
685

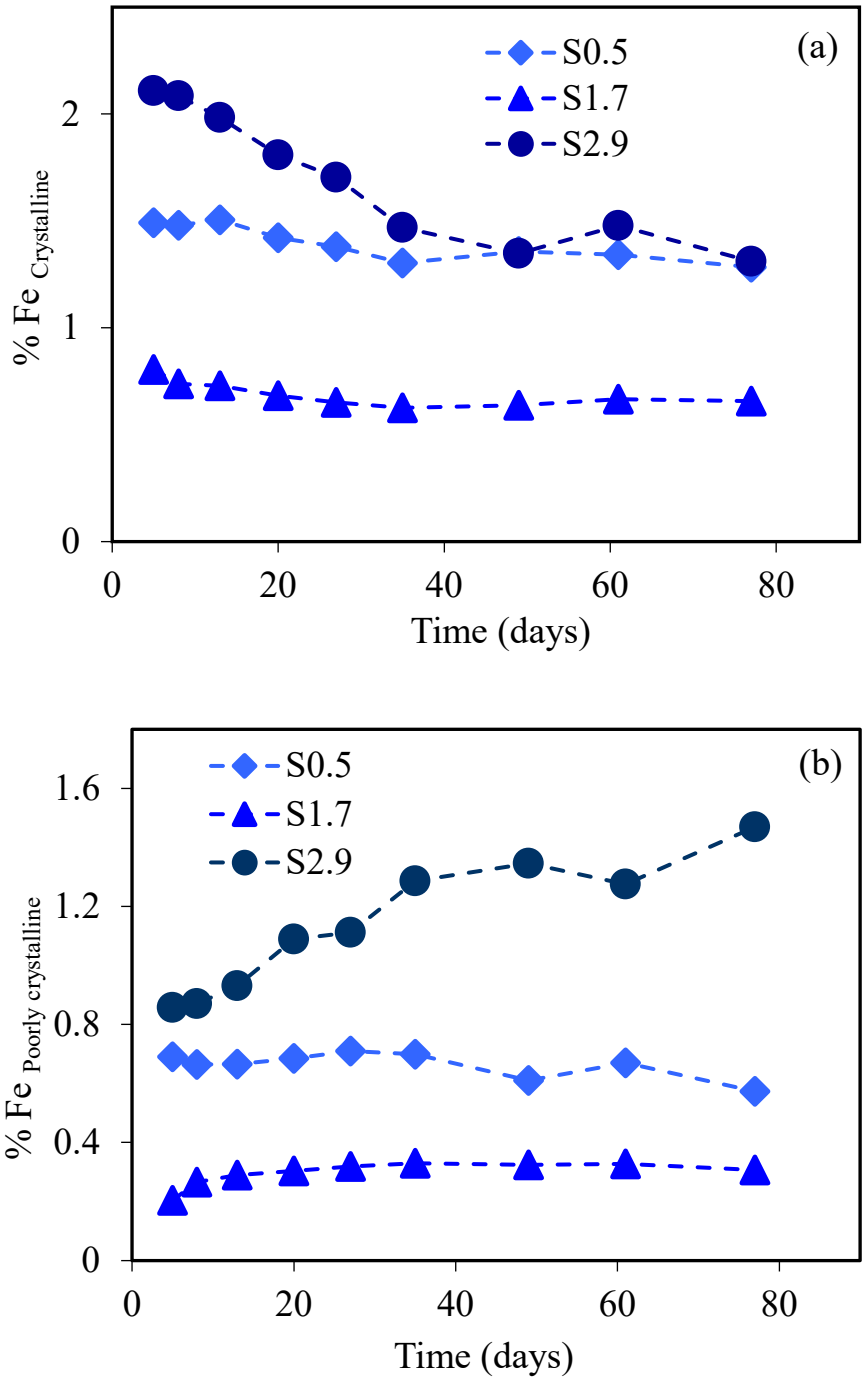

686
687
688
689 **Fig.3.** Effect of flooding time on the percentage (g/100g soil) of a) crystalline and b) poorly crystalline
690 iron in $S_{0.5}$, $S_{1.7}$ and $S_{2.9}$ soil samples under anoxic conditions

691

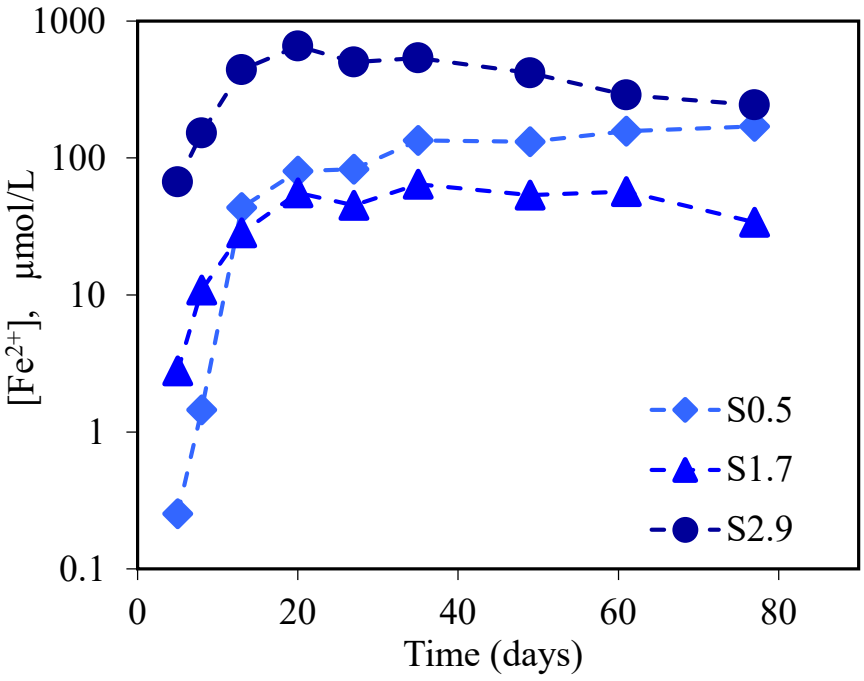

Fig. 4. Effect of flooding time on the concentration of ferrous iron (µmol/L) in $S_{0.5}$, $S_{1.7}$ and $S_{2.9}$ soil samples under anoxic conditions

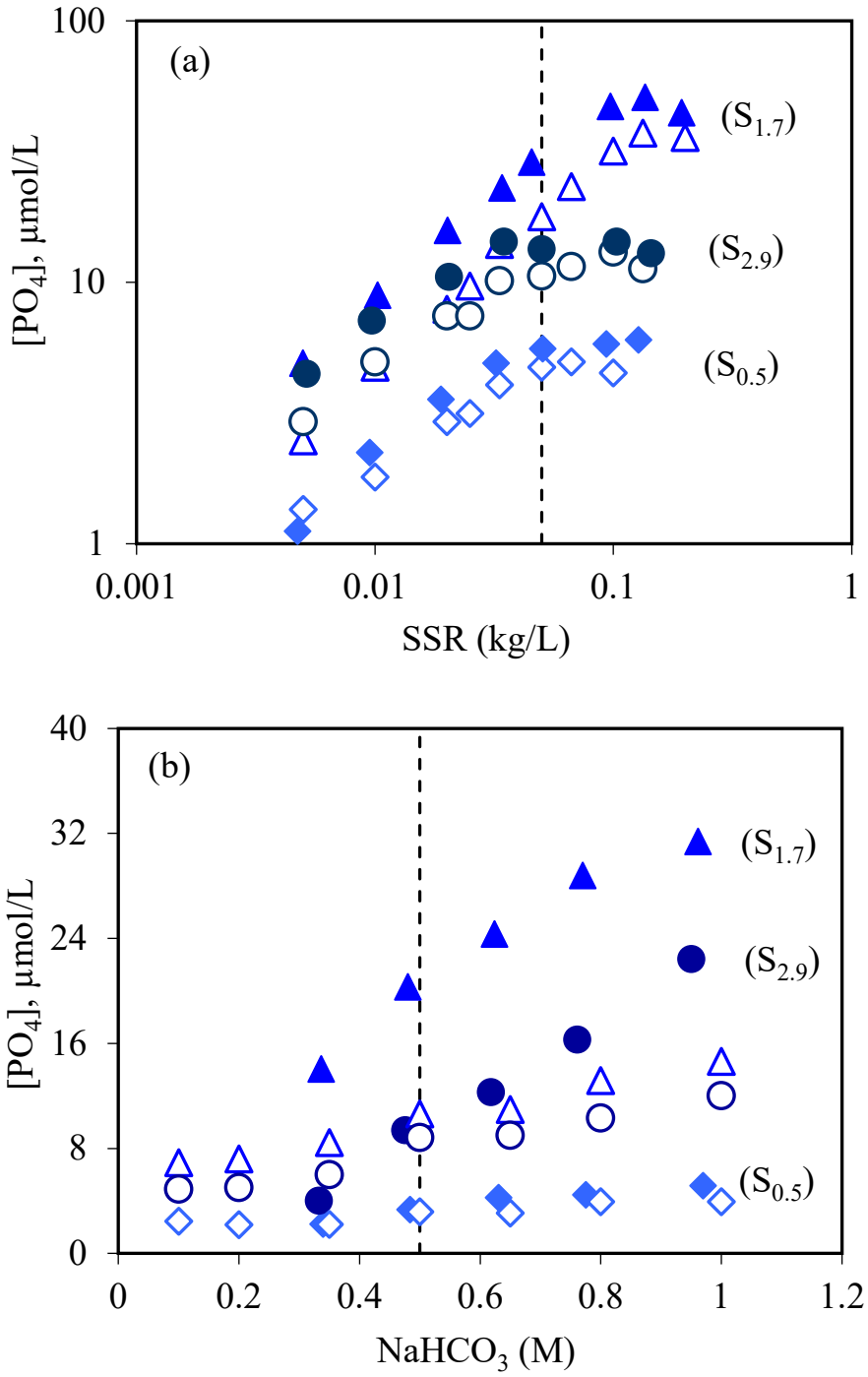

706 **Fig 5.** a) Effect of SSR on extractable P in soil under oxic (empty symbols) and anoxic (solid symbols)
707 conditions. The vertical dashed line corresponds to the SSR used in the standard Olsen-P method (i.e. SSR
708 = 1:20). The equilibration time in these experiments was 180 min, rather than 30 min that is used in the
709 standard Olsen method. b) Effect of sodium bicarbonate concentration on the concentration of extracted
710 phosphate from soil under oxic (empty symbols) and anoxic (solid symbols) conditions. The vertical dashed
711 line corresponds to the sodium bicarbonate concentration in the standard Olsen-P method (0.5 M).

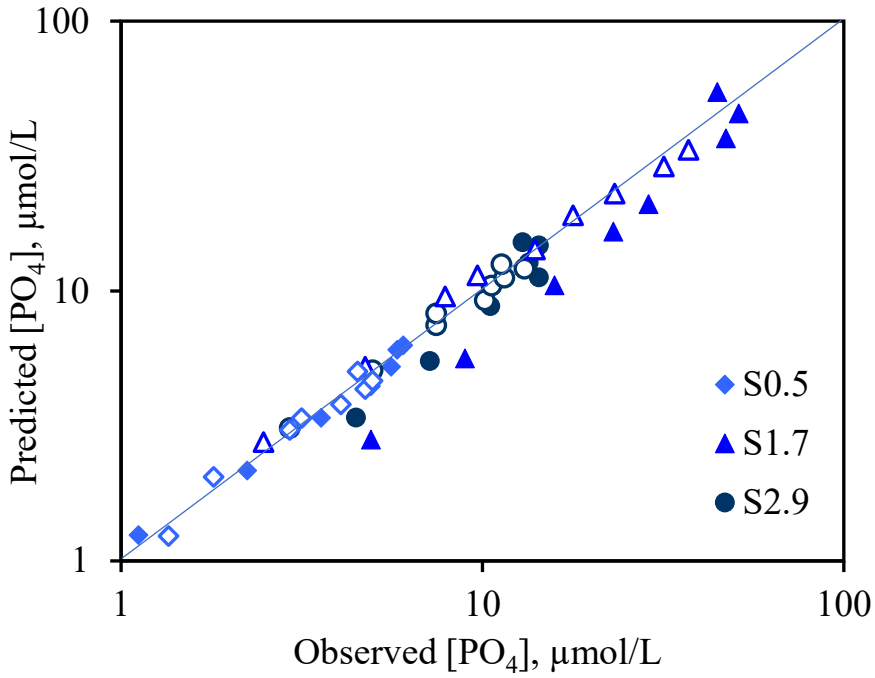

Fig 6. Model predictions vs experimental observations for the effect of SSR (1:5, 1:7.5, 1:10, 1:15, 1:20, 1:30, 1:40, 1:50, 1:100 and 1:200 kg/L) on extractable P in soil under oxic (empty symbols) and anoxic (solid symbols) conditions. The predictions were calculated using the CD-MUSIC model, as described in section 2.5. The solid line represents the reference 1:1 line. All the data are within the two-times RMSE (equal to 6.06, which was calculated based on (Groenenberg et al. 2017).